Electronic Supplementary Material

Theoretical study on Janus graphene oxide membrane for water transport

Quan Liu[1], Mingqiang Chen[1], Yangyang Mao[2], Gonging Liu (✉)[2]

1 Analytical and Testing Center, Anhui University of Science and Technology, Huainan 232001, China

2 State Key Laboratory of Materials-Oriented Chemical Engineering, College of Chemical Engineering, Nanjing Tech University, Nanjing 211816, China
E-mail: gpliu@njtech.edu.cn

The GO models were firstly subjected to energy minimization in Materials Studio 6.0. The energy has been converged after 800 iterations in Fig. S1. And the most stable orientation was achieved by the model of OPOP (or POPO).

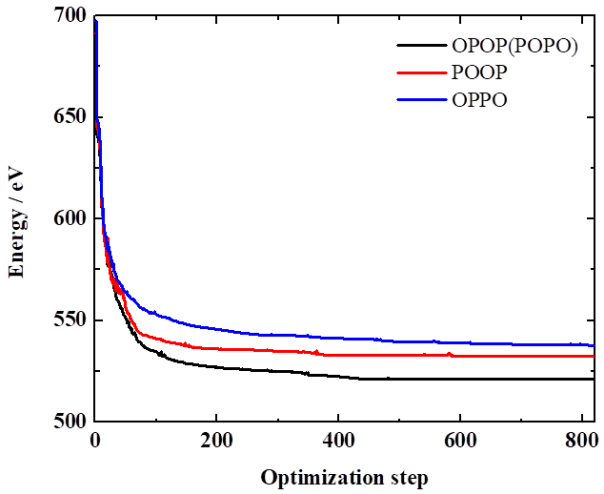

Fig. S1. Energy minimization of Janus GO models.

The radial distribution function [1] (RDF, equation S1) was used to analyze the affinity of four Janus GO membranes to water molecules. The OPOP membrane exhibited a slightly higher affinity toward water molecules, even though the difference of RDF curves was unobvious because of the uniform oxidized degree. Additionally, the first peak of four RDF in Fig. S2a is all around r = 0.45 nm, which is an indicator of the first adsorption layer of water on GO surface. Water density contours on the cross-section of GO membranes showed that there was a water sorption layer with a thickness of 0.45 nm on the GO membrane, as shown in Fig. S2b.

$$g_{ij}(r) = \frac{N_{ij}(r,r+\Delta r)V}{4\pi r^2 \Delta r N_i N_j} \quad \text{(S1)}$$

where r is the distance between atom species i and j, N_i is the number of atom i, and N_{ij} $(r, r+\Delta r)$ refers to the number of species j around i within a shell.

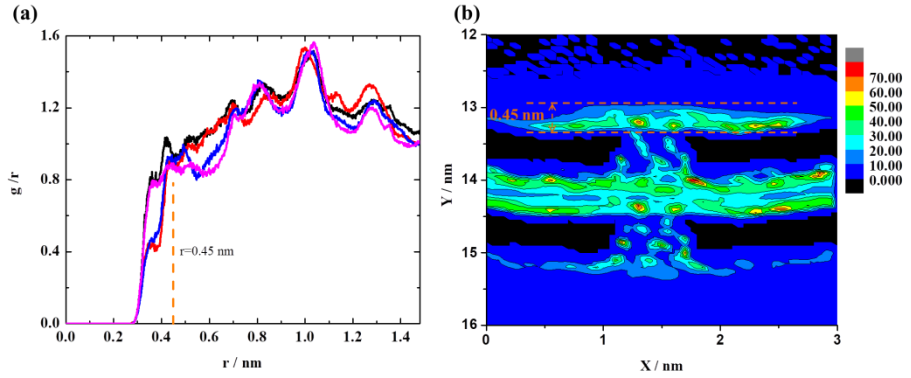

Fig. S2. (a) Radial distribution functions of water around Janus GO membranes; (b) The water density contours on the cross-section of GO membrane. The unit of density (N_w/uc) is 1/(1.25Å^3).

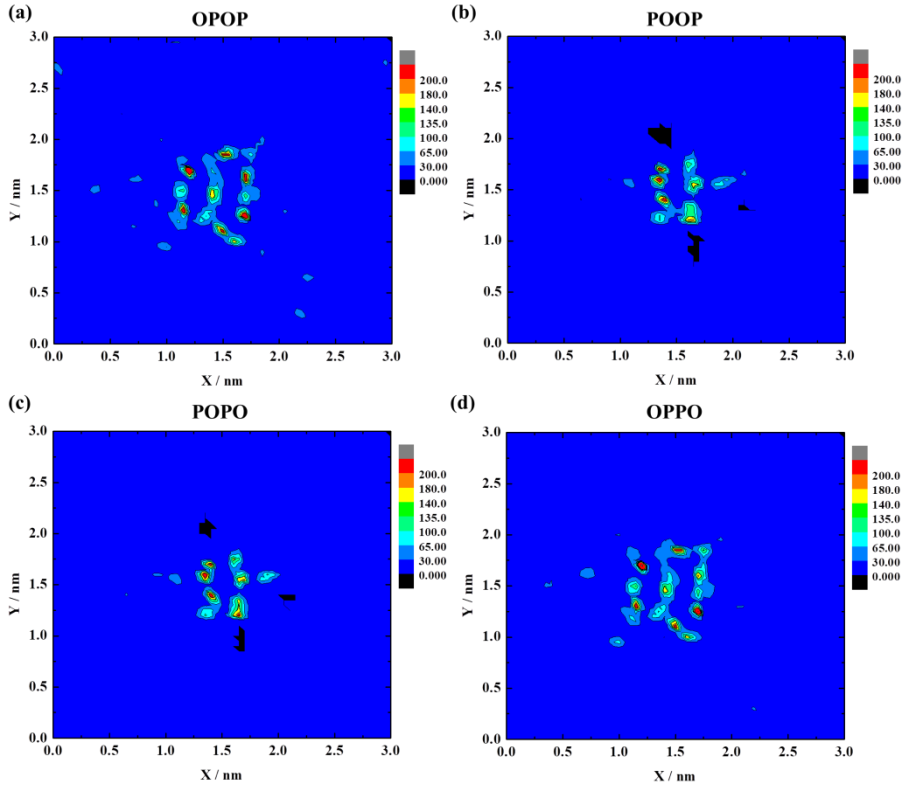

Fig. S3. Density contours of water on GO membranes. The unit of density (N_w/uc) is 1/(1.25Å^3).

To understand the effect of the upper surface on water permeation, we calculated water density counters on GO membranes. Clearly, water molecules were highly assembled in pore's territory in Fig. S3 due to the primary pathway of pore

penetration. Note that the hydrophilic upper surface was more likely to drag water in pores [2] where the water density was relatively high (180–200 Nw/uc), as shown in Fig. S3a and 3d. The partially oxidized channels promoted the pore-to-pore transport with large vertical diffusion in the OPOP membrane. However, the pristine interlayer in the OPPO membrane had the lowest vertical water diffusion coefficient in Fig. 4b. So higher water flux in OPOP than in OPPO should be ascribed to the fast vertical diffusion of water molecules in columnar pores.

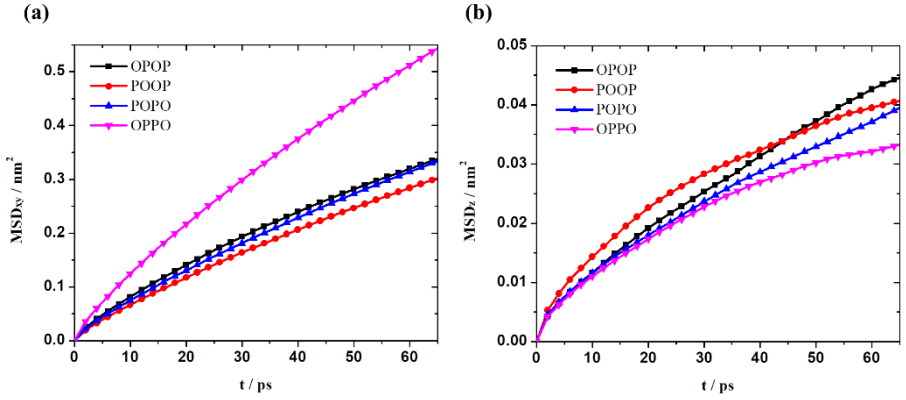

Fig. S4. MSD curves of water molecules accommodated in GO interlayers. (a) Lateral diffusion; (b) Vertical diffusion.

Mean square displacements (MSD) of lateral and vertical diffusions are presented in Fig. S4. For the pristine channel built-in OPPO membrane, hydrophobic carbons enchanted water to wander in the extended interlaminar pathway with little resistance, resulting in the fastest lateral movement in Fig. S4a but the lowest vertical movement in Fig. S4b. The interlaminar water movement would suffer more resistance with the increased oxygen-containing groups [3]. Therefore, lateral MSD values decreased as follows: $MSD_{(OPPO)} > MSD_{(OPOP)} \approx MSD_{(POPO)} > MSD_{(POOP)}$ in Fig. S4a. However, for the oxidized channel in the OPOP membrane, more resistance generated in the interlaminar pathway that pushed water to select the other approach to directly cross the membrane, namely, the pore-to-pore transport. The tendency of lateral MSD went into sharp reverse in Fig. S4b. Especially during the initial correlation time, the vertical movement through columnar pores was in the order: $MSD_{(POOP)} > MSD_{(OPOP)} > MSD_{(POPO)} > MSD_{(OPPO)}$. Because the oxidized channels stimulated pore-to-pore transport while restraining the extended interlaminar movement. The increased functional groups needed more time to equilibrate the

molecules, which might reduce the vertical water diffusion in the POOP membrane. Additionally, more water was captured into the first pore by the oxidized upper surface, which further accelerated the vertical diffusion of water in OPOP membrane. As a result, with larger correlation time, the vertical movement through columnar pores increased as follows: $MSD_{(OPPO)} < MSD_{(POPO)} < MSD_{(POOP)} < MSD_{(OPOP)}$.

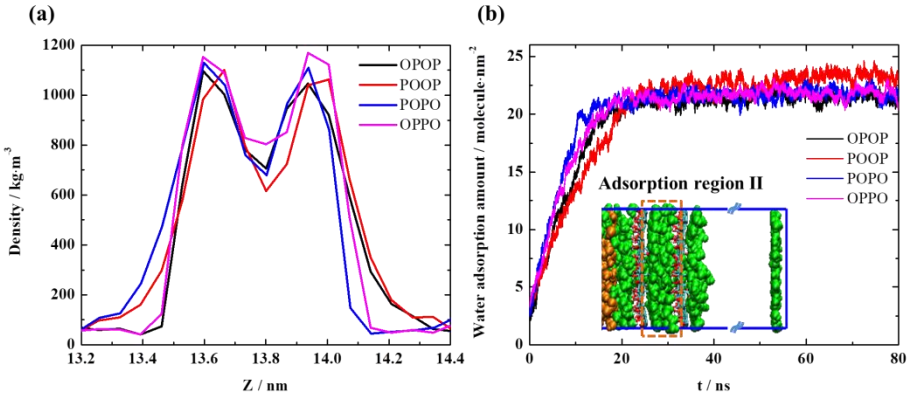

Fig. S5. Water accommodated in GO interlayers. (a) The mass density; (b) The water adsorption amount. (Inset) Water adsorption region II with a thickness of 1.2 nm in the interlayer marked by the yellow rectangle.

Two water layers were formed once the water entered into the interlayers (see Fig. S5a), which thoroughly freed water's diffusion. For the OPOP membrane, the hydrophilic upper surface captured water into the interlayer [2], and then the partially oxidized channel endowed water with fast vertical but slow lateral diffusion. As a result, water molecules performed the pore-to-pore transport directly in the OPOP membrane, as marked by the blue rectangle in Fig. S6a. So the OPOP membrane had desirable microstructures to inspire a directed pore penetration for water molecules and avoid the extended pathway in interlayers. With the fixed interlayer distance of 1.2 nm, the adsorption region II was marked by the yellow rectangle (Fig. S5b, inset). The water adsorption amount in interlayer was calculated by the command "gmx select" provided by Gromacs which could select the number of water atoms in interlayers. As shown in Fig. S5b, the results showed that the water adsorption amounts in these four interlayers were almost the same, implying the important effect of the upper surface on preferential water adsorptions.

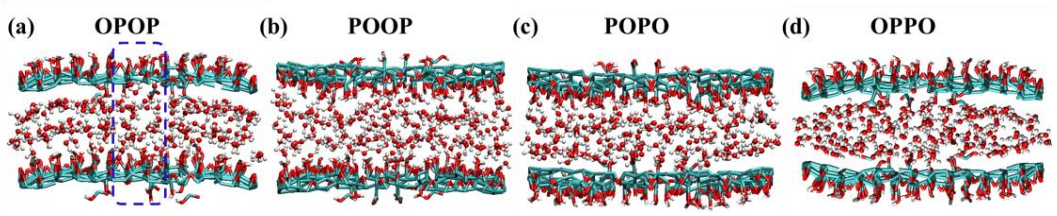

Fig. S6. Equilibrium snapshots of water in GO interlayers.

In GO interlayers, hydrogen bonds were also examined in Fig. S7 based on the two geometrical criteria [4, 5]: (1) r(H···O) ≤ 0.35 nm; (2) α(O-H···O) ≤ 30°. On average, one water molecule formed about 3.2 hydrogen bonds in interlayers, which was greater than that of feed tank (3.0), as shown in Fig. S7a. With more oxidized regions, hydrogen bonds between the water and interlayer were easier to be formed, as exhibited in Fig. S7b, resulting in a clear decreasing trend as follows: POOP > POPO ≈ OPOP > OPPO. These hydrogen bonds also affected water flux.

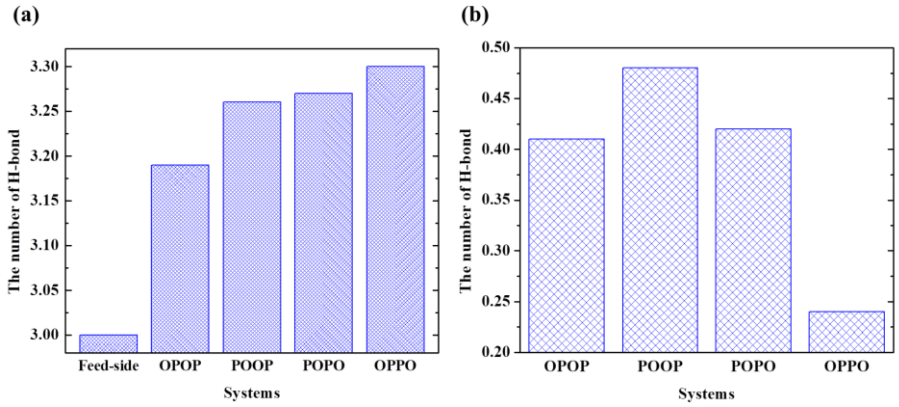

Fig. S7. The average number of hydrogen bonds per water molecule in interlayers. (a) Water-water; (b) Water-interlayers.

The potential of mean force (PMF) is a good way to study the permeation behavior of water. It was calculated according to the following equation S2 [6,7], where T is the temperature, R is the gas constant, and $\rho(bulk)$ and $\rho(z)$ refer to the number density profiles of water in the bulk solution and perpendicular to the interface, respectively. As presented in Fig. S8, water molecules crossed four Janus GO membranes with two energy barriers. In detail, at the first saddle point, the membranes with an oxidized upper surface (OPOP and OPPO) had a relatively lower energy barrier for water permeating. It was the same at the second saddle point,

primarily because the oxidized upper surfaces had more attractive to water molecules and generated low energy barrier for them to overwhelm. When two GO nanosheets are supposed to be connected in series, the total energy barrier ($E_I + E_{II}$) is the sum of each one. Absolutely, with double oxidized upper surfaces, the total energy barrier for water crossing OPOP membrane was the lowest among four Janus GO membranes.

$$G_z = -RTln\frac{\rho(z)}{\rho(bulk)} \qquad (S2)$$

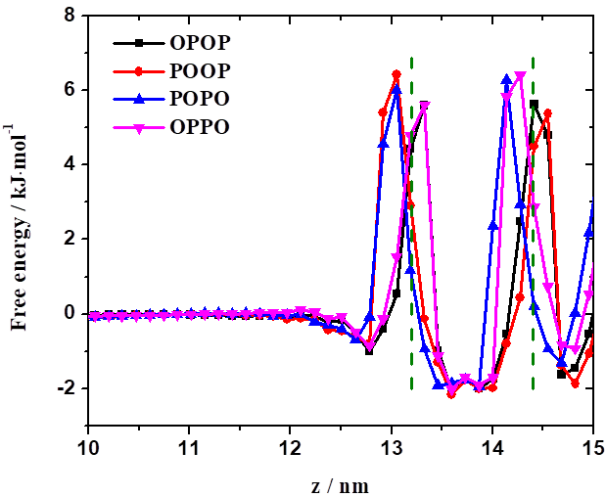

Fig. S8. The PMF of water molecules permeating through GO membranes. GO membranes are located at the green dotted lines.

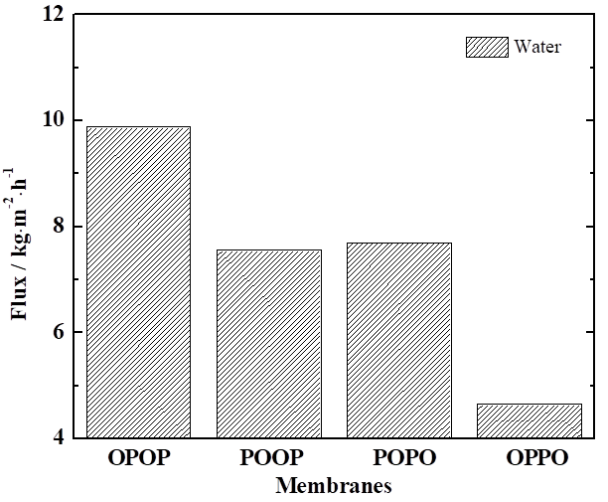

Fig. S9. Water flux of 50 wt% water–ethanol mixture through four Janus GO membranes.

Finally, the separation of 50 wt% water–ethanol mixture through Janus GO membranes was also simulated. A similar decreasing trend (OPOP > POOP ≈

POPO > OPPO) of water flux was reproduced in Fig. S9. No matter what the concentration of the water–ethanol mixture was, the OPOP membrane achieved the largest water permeability, while the OPPO presented the lowest.

References

1. Chen T-H, Chen Y-R, Chen L-H, Chang K-S, Lin Y-F, Tung K-L. Exploration of the nanostructures and separation properties of cross-linked mixed matrix membranes using multiscale modeling. Journal of Membrane Science, 2017, 543: 328–334
2. Huang K, Liu G, Lou Y, Dong Z, Shen J, Jin W. A graphene oxide membrane with highly selective molecular separation of aqueous organic solution. Angewandte Chemie-International Edition, 2014, 53(27): 6929–6932
3. Chen B, Jiang H, Liu X, Hu X. Observation and analysis of water transport through graphene oxide interlamination. Journal of Physical Chemistry C, 2017, 121(2): 1321–1328
4. Gupta K M, Liu J, Jiang J. A molecular simulation protocol for membrane pervaporation. Journal of Membrane Science, 2019, 572: 676–682
5. Zhao D, Liu J, Jiang J. Porous organic cages embedded in a lipid membrane for water desalination: A molecular simulation study. Journal of Membrane Science, 2019, 573: 177–183
6. Sedlmeier F, von Hansen Y, Mengyu L, Horinek D, Netz R R. Water dynamics at interfaces and solutes: Disentangling free energy and diffusivity contributions. Journal of Statistical Physics, 2011, 145(2): 240–252
7. Wang Y, He Z, Gupta K M, Shi Q, Lu R. Molecular dynamics study on water desalination through functionalized nanoporous graphene. Carbon, 2017, 116: 120–127